Flores, P., Lankarani, H.M., Spatial rigid-multi-body systems with lubricated spherical clearance joints: modeling and simulation. Nonlinear Dynamics, Vol. 60(1-2), pp. 99-114, 2010, (DOI: 10.1007/s11071-009-9583-z)

Paulo Flores[1*] and Hamid M. Lankarani[2]

[1] Department of Mechanical Engineering, University of Minho
Campus de Azurém, 4800-058 Guimarães, Portugal

[2] Department of Mechanical Engineering, Wichita State University
Wichita, KS 67260-133, USA

Abstract

The dynamic modeling and simulation of spatial rigid-multi-body systems with lubricated spherical joints is the main purpose of the present work. This issue is of paramount importance in the analysis and design of realistic multibody mechanical systems undergoing spatial motion. When the spherical clearance joint is modeled as dry contact; i.e., when there is no lubricant between the mechanical elements which constitute the joint, a body-to-body (typically metal-to-metal) contact takes place. The joint reaction forces in this case are evaluated through a Hertzian-based contact law. A hysteretic damping factor is included in the dry contact force model to account for the energy dissipation during the contact process. The presence of a fluid lubricant avoids the direct metal-to-metal contact. In this situation, the squeeze film action, due to the relative approaching motion between the mechanical joint elements, is considered utilizing the lubrication theory associated with the spherical bearings. In both cases, the intra-joint reaction forces are evaluated as functions of the geometrical, kinematical and physical characteristics of the spherical joint. These forces are then incorporated into a standard formulation of the system's governing equations of motion as generalized external forces. A spatial four bar mechanism that includes a spherical clearance joint is considered here as example. The computational simulations are carried out with and without the fluid lubricant, and the results are compared with those obtained when the system is modeled with perfect joints only. From the general results it is observed that the system's performance with lubricant effect presents fewer peaks in the kinematic and dynamic outputs, when compared with those from the dry contact joint model.

Keywords: Lubricated Spherical Clearance Joints, Dry Contact, Spatial Multibody Dynamics

* Corresponding author: e-mail: pflores@dem.uminho.pt

1. Introduction

The main objective of this study is to present a general and comprehensive methodology for modeling and simulating of realistic spherical joints with clearances under the framework of multibody systems methodologies. The motivation for this research work comes from current interest in developing mathematical and computational tools for the dynamics of multibody systems in which the effects of clearance, surface compliance, friction and lubrication in real joints are taken into account [1-6]. These phenomena can be included in a multibody system with a spherical joint, and in many applications the function of the mechanical systems strongly depends on them. Typical examples are the spherical joints of a vehicle steering suspension and the artificial hip implants. In the vehicle example, either due to the loads carried by the system or misalignments that are required for their operations, real spherical joints must be lubricated or include bushing elements, generally made with metals or polymers. By using rubber bushings, a conventional mechanical joint is transformed into a joint with clearance allowing for the mobility of the over-constrained system in which it is used [7, 8]. In the example of artificial hip articulations, some amount of clearance is always necessary to allow the assembly of the femoral head and acetabular cup and to facilitate the system's operation. Hip implants are in fact the most typical application of lubricated spherical joints in which the knowledge of the clearance size and external load are of great importance for their dynamic performances. Most of the available literature on this subject is mostly formulated on the tribological level, in the measure that the geometrical properties (e.g., clearance size) of the hip implants are not considered as variables. The kinematic (e.g., angular velocities) and dynamic (e.g., applied forces) characteristics of the hip elements are also assumed to be constant in most of the studies [9-11]. Nevertheless, these quantities vary during any daily human activity.

Mechanical joints of any industrial machine allow the relative motion between the components connected by them. Due to the manufacturing tolerances, wear or material deformation, these joints are imperfect and have clearances. These clearances modify the dynamic response of the system, justify the deviation between the numerical and experimental measurements, and eventually lead to important deviations between the projected behavior of the mechanisms and their real outcome. The attenuation of the impact response and of vibration characteristics in industrial machines can be obtained by including, in their design, a selection of joint clearance. The imperfect joints with direct contact between the involved parts generally use lubrication to minimize the energy dissipation. Therefore, appropriate tribological models must be devised in the framework of their application in general mechanical systems.

On the subject of clearance and lubrication joints, research works mostly deal with planar multibody systems. Dubowsky and Freudenstein [12] formulated an impact pair model to predict the dynamic response of an elastic mechanical joint with clearance. In their model, springs and dashpots were arranged as linear spring-damper type Kelvin-Voigt model. Dubowsky [13] showed how clearances can interact dynamically with machine control systems to destabilize and produce undesirable limit cycle behavior. Earles and Wu [14] employed a modified Lagrange's equation approach in which constraints were incorporated using Lagrange multipliers in order to predict the behavior of rigid-body mechanism with clearance in a journal-bearing. The clearance in the journal-bearing was modeled by a massless imaginary link, but the simulation was restricted to the range of motion that starts when the contact between the journal and the bearing is terminated. Grant and Fawcett [15] proposed a method to prevent contact-loss between the journal and bearing. Their experimental results verified the approach for a limited class of systems, however, the method is not universal [16]. Townsend and Mansour [17] modeled a four bar crank-rocker mechanism with clearance as two sets of

compound pendulums in a theoretical study. The motion in contact mode was ignored entirely in this study, a close succession of small pseudo-impacts was assumed for the simulation. Subsequently, Miedema and Mansour [18] extended their previous two-mode model, for the free-flight and impact modes, to a three mode model in which a follower or continuous mode was proposed. In their numerical simulations, the follower mode was always assumed to occur immediately after the impact mode; however, this is frequently not observed in practice. Haines [19] derived equations of motion that describe the contributions at a revolute joint with clearance but with no lubrication present. Bengisu et al. [20] developed a separation parameter for a four-bar linkage which was based on a zero-clearance analysis. The theoretical results were compared with the experimental results and showed a qualitative agreement.

More recently, Feng et al. [21] developed an optimization method to control the change of inertia forces by optimizing the mass distribution of moving links in planar linkages with clearances at joints. Orden [22] presented a methodology for the study of typical smooth joint clearances in mechanical systems. This proposed approach takes advantage of the analytical definition of the material surfaces defining the clearance, resulting in a formulation where the gap does not play a central role, as it happens in standard contact models. Other researchers also included the influence of the flexibility of the bodies in the dynamic performance of mechanical systems besides the existence of gaps in the joints [23-25]. Dubowsky and Moening [26] obtained a reduction in the impact force level by introducing flexibility of the bodies. They also observed a significant reduction of the acoustical noise produced by the impacts when the system incorporates flexible bodies. Kakizaki et al. [27] presented a model for spatial dynamics of robotic manipulators with flexible links and joint clearances, where the effect of the clearance is taken to control the robotic system.

Almost all the aforementioned studies on the dynamic performance of multibody systems with real joints are only valid for two dimensional systems. Liu et al. [28] developed a simple contact force formulation of the spherical clearance joints in multibody mechanical systems, using the distributed elastic forces to model the compliant of the surfaces in contact. Flores et al. [29] also presented a methodology to assess the influence of the spherical joint clearances in spatial multibody systems. Both of these approaches are only valid for the case of dry contact between the socket and the ball. Thus, the present work deals with the dynamic modeling and analysis of spatial multibody systems with lubricated spherical joints. This paper extends previous authors' work [29] to include the lubrication action into the spherical joints. In a simple way, the intra-joint forces developed at the dry and lubricated spherical joints are evaluated as functions of geometrical, kinematical and physical properties of the joint elements. For these purposes, two different approaches are employed. For the dry contact situation, the joint contact-impact forces are computed by using a continuous constitutive contact force law based on the Hertz theory. The energy-dissipative effect associated with the contact-impact process is included by a hysteresis-type damping term. For the case in which a fluid lubricant exists between the joint elements, the squeeze lubrication action is modeled employing the hydrodynamic lubrication theory. The aim here is to evaluate the resulting forces from the given state of position and velocity of the spherical bearings. For both cases, the joint reaction forces are introduced into the equations of motion as external applied forces [30-36]. Finally, results for a spatial four bar mechanism with a lubricated spherical clearance joint are presented to discuss the main assumptions and procedures adopted throughout this work.

2. Kinematics of spherical joints

In order to characterize the real joints, it is necessary to develop a mathematical model for spherical clearance joints in the multibody mechanical systems. In standard multibody models, it is assumed that the connecting points of two bodies, linked by an ideal spherical joint, are coincident. The introduction of the clearance in a spherical joint separates these two points and the bodies became free to move relative to one another. A spherical joint with clearance does not constrain any degree-of-freedom (DOF) from the system like an ideal spherical joint. In a spherical clearance joint, the dynamics of the joint is controlled by contact-impact forces which result from the collision between the connected bodies. Thus, this type of joint can be called as force-interaction-joint, since it deals with force effects rather than the kinematic constraints.

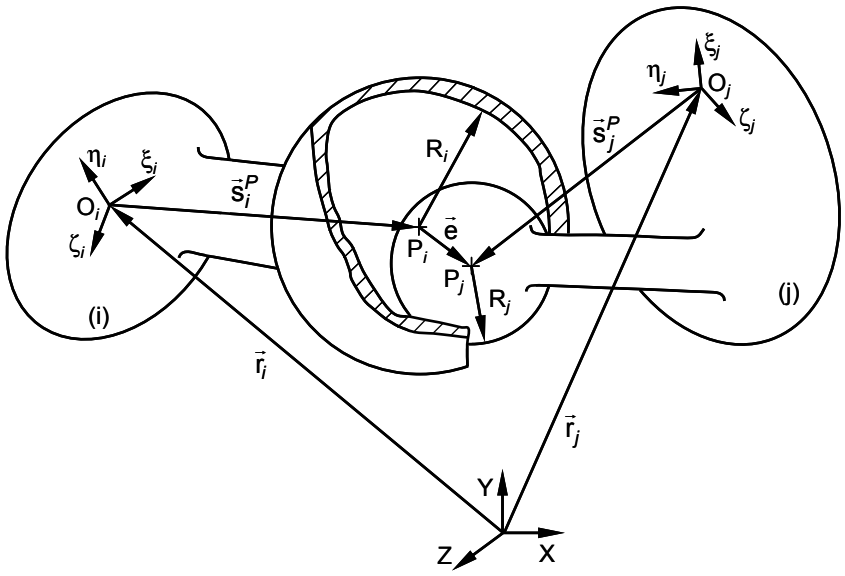

Figure 1. General configuration of a spherical clearance joint in a multibody system.

Figure 1 depicts two bodies *i* and *j* connected by a spherical joint with clearance. A spherical part of body *j*, the ball, is inside of a spherical part of body *i*, the socket. The radii of socket and ball are R_i and R_j, respectively. The difference in radius between the socket and the ball defines the size of radial clearance, $c=R_i-R_j$. The centers of mass of bodies *i* and *j* are O_i and O_j, respectively. Body-fixed coordinate systems $\xi\eta\zeta$ are attached at their centers of mass, while *XYZ* represents the global inertial frame of

reference. Point P_i indicates the center of the socket, while the center of the ball is denoted by P_j. The vector that connects the point P_i to point P_j is defined as the eccentricity vector, which is represented in Fig. 1. Note that, in real systems, the magnitude of the eccentricity is typically much smaller than the radius of the socket and ball [37].

In what follows, some of the most relevant kinematic aspects related to the spherical clearance joint are presented. As displayed in Fig. 1, the eccentricity vector **e**, which connects the centers of the socket and the ball, is given by,

$$\mathbf{e} = \mathbf{r}_j^P - \mathbf{r}_i^P \tag{1}$$

where both $\mathbf{r}_j^P$ and $\mathbf{r}_i^P$ are described in global coordinates with respect to the inertial reference frame [30],

$$\mathbf{r}_k^P = \mathbf{r}_k + \mathbf{A}_k \mathbf{s}'^P_k, \quad (k=i,j) \tag{2}$$

The magnitude of the eccentricity vector is evaluated as,

$$e = \sqrt{\mathbf{e}^T \mathbf{e}} \tag{3}$$

The magnitude of the eccentricity vector expressed in the global coordinates is written as [30],

$$e = \sqrt{(x_j^P - x_i^P)^2 + (y_j^P - y_i^P)^2 + (z_j^P - z_i^P)^2} \tag{4}$$

and the time rate of change of the eccentricity in the radial direction, that is, in the direction of the line of centers of the socket and the ball is,

$$\dot{e} = \frac{(x_j^P - x_i^P)(\dot{x}_j^P - \dot{x}_i^P) + (y_j^P - y_i^P)(\dot{y}_j^P - \dot{y}_i^P) + (z_j^P - z_i^P)(\dot{z}_j^P - \dot{z}_i^P)}{e} \tag{5}$$

in which the dot denotes the derivative with respect to time.

A unit vector **n** normal to the collision surface between the socket and the ball is aligned with the eccentricity vector, as observed in Fig. 2. Thus, it can be stated that

$$\mathbf{n} = \frac{\mathbf{e}}{e} \tag{6}$$

Figure 2 illustrates the situation in which the socket and the ball bodies are in contact, which is identified by the existence of a relative penetration, δ. The contact or control points on bodies i and j are Q_i and Q_j, respectively. The global position of the contact points in the socket and ball are given by [30],

$$\mathbf{r}_k^Q = \mathbf{r}_k + \mathbf{A}_k \mathbf{s}_k'^Q + R_k \mathbf{n}, \quad (k=i,j) \tag{7}$$

where R_i and R_j are the socket and ball radius, respectively.

The velocities of the contact points Q_i and Q_j in the global system are obtained by differentiating Eq. (7) with respect to time, yielding,

$$\dot{\mathbf{r}}_k^Q = \dot{\mathbf{r}}_k + \dot{\mathbf{A}}_k \mathbf{s}_k'^Q + R_k \dot{\mathbf{n}}, \quad (k=i,j) \tag{8}$$

Let the components of the relative velocity of contact points in the normal and tangential direction to the surface of collision represented by $\mathbf{v}_N$ and $\mathbf{v}_T$, respectively. The relative normal velocity determines whether the bodies in contact are approaching or separating, and the relative tangential velocity determines whether the bodies in contact are sliding or sticking [38]. The relative scalar velocities, normal and tangential to the surface of collision, v_N and v_T, are obtained by projecting the relative impact velocity onto the tangential and normal directions, yielding,

$$\mathbf{v}_N = [(\dot{\mathbf{r}}_j^Q - \dot{\mathbf{r}}_i^Q)^T \mathbf{n}]\mathbf{n} \tag{9}$$

$$\mathbf{v}_T = (\dot{\mathbf{r}}_j^Q - \dot{\mathbf{r}}_i^Q)^T - \mathbf{v}_N \equiv v_T \mathbf{t} \tag{10}$$

where $\mathbf{t}$ represents the tangential direction to the impacted surfaces.

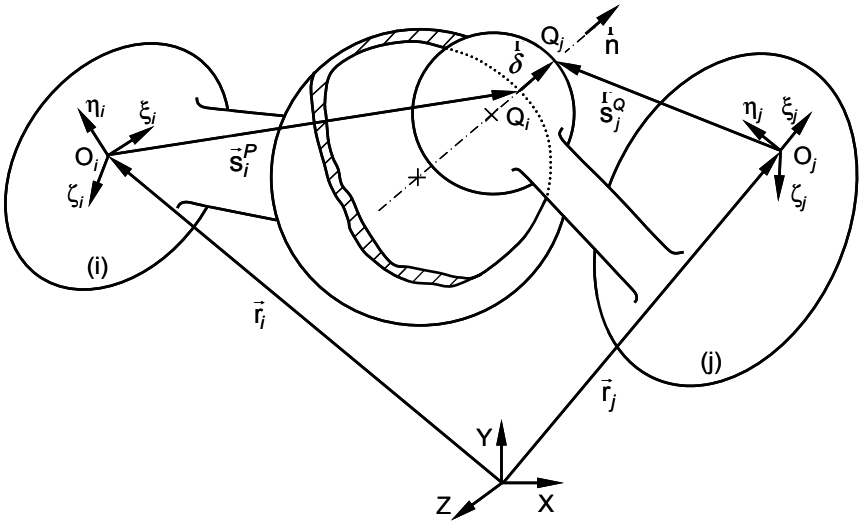

Figure 2. Penetration depth between the socket and the ball during the contact.

From Fig. 2 it is clear that the geometric condition for contact between the socket and ball can be defined as,

$$\delta = e - c \tag{11}$$

where e is the magnitude of the eccentricity vector given by Eq. (3) and c is the radial clearance size. It should be noted that here the clearance is taken as a specified parameter. When the magnitude of the eccentricity vector is smaller than the radial clearance size, there is no contact between the socket and the ball, and consequently, they can freely move relative to each other. When the magnitude of eccentricity is larger than radial clearance, there is contact between the socket and ball, being the relative penetration given by Eq. (11). The contact problem studied within the framework of multibody systems formulations can be divided into two main phases, namely (i) the contact detection and (ii) the application of an appropriate contact force law. The contact detection is the procedure which allows to check whether the potential contacting surfaces are in contact or not. For multibody systems this analysis is performed by evaluating, at each integration time step, the gap or distance between contacting points. When this distance is negative it means that the bodies overlap, and hence in these situations, the distance is designated as penetration or indentation. In realty, the bodies do not penetrate

each other, but they deform. In computational simulations the penetration is related to the actual deformation of the bodies. On the other hand, in the second phase of the contact modeling problems, the application of the contact law deals with the use of an appropriate constitutive law relating the penetration and the contact forces necessary to avoid the inter-penetration of the contacting bodies. In other words, the contact force can be thought of penalizing the pseudo-penetration, and hence this approach is commonly denominated as penalty method.

Finally, when the space between the ball and socket is filled with a lubricant, the joint becomes a spherical joint with lubrication action, whose kinematic are aspects similar to those for the spherical joint with clearance. The only difference is that the relative radial velocity expressed by Eq. (8) leads the lubricant squeeze action when there is no contact between the ball and socket walls.

3. Dynamics of spherical joints

The main issues related to the dynamics of spherical joint with dry clearance and lubrication are presented in this section. Hence, the dry contact and lubricant forces are formulated in the framework of multibody systems methodologies. In both cases, the forces developed at the spherical joints are introduced into the system's equations of motion as external generalized forces.

When there is no lubricant in the joint, an internal impact takes place in the system and the corresponding impulse is transmitted throughout the multibody system. Contact-impacts of such occurring within a spherical clearance joint, are one of the most common types of dynamic loading conditions which give rise to impulsive forces, and in turn excite higher vibration modes and affect the dynamic characteristics of the mechanical system. For a spherical joint with clearance, the contact between the socket and the ball can be modeled by the well known Hertz contact law [39],

$$F_N = K\delta^n \tag{12}$$

where K is the generalized stiffness constant and δ is the relative normal deformation between the spheres. The exponent n is set to 1.5 for the cases where there is a parabolic distribution of contact stresses, as in the original work by Hertz. The parameter K is dependent on the material properties and the shape of the contact surfaces. For two spheres in contact, the generalized stiffness coefficient is a function of the radii of the spheres i and j and the material properties as [40],

$$K = \frac{4}{3(\sigma_i + \sigma_j)}\left[\frac{R_i R_j}{R_i + R_j}\right]^{\frac{1}{2}} \tag{13}$$

where the material parameters σ_i and σ_j are given by,

$$\sigma_k = \frac{1-\nu_k^2}{E_k}, \quad (k=i,j) \tag{14}$$

and the quantities ν_k and E_k are the Poisson's ratio and the Young's modulus associated with each sphere, respectively. Hertz contact law given by Eq. (12) is a pure elastic model, i.e., it does not include any energy dissipation. Lankarani and Nikravesh [41, 42] extended the Hertz contact law to include energy loss due to internal damping as follows,

$$F_N = K\delta^n \left[1 + \frac{3(1-c_r^2)}{4} \frac{\dot{\delta}}{\dot{\delta}^{(-)}} \right] \tag{15}$$

in which the generalized parameter K is evaluated by Eqs. (13) and (14) for sphere to sphere contact, c_r is the restitution coefficient, $\dot{\delta}$ is the relative penetration velocity and $\dot{\delta}^{(-)}$ is the initial impact velocity.

It is known that in some applications of multibody systems, the spherical joints are designed to operate with some lubricant fluid, and hence, the space between the socket and ball surfaces is filled with a lubricant. The pressure level generated in the lubricant act to keep the socket and ball surfaces apart. Additionally, the film formed by the lubricant reduces friction and wear, and provides load capacity and adds damping to dissipate undesired mechanical vibrations.

In a broad sense, dynamically loaded spherical joints can be classified into two main groups, namely the squeeze-film action and the wedge-film action [43-50]. The first group refers to the situations in which the ball does not rotate significantly about its center, rather the ball moves along some path inside the socket boundaries. The second group deals with cases for which the ball has significant rotation, typical of very high-speed rotating machinery. In a spherical joint, the squeeze-film action is dominant when the relative rotational velocity between the ball and the socket is small compared to the relative radial velocity. When the relative rotational velocity is high, the wedge-film effect must also be taken into account. In the methodology presented in this study, the squeeze-film effect is the only lubrication action considered. This phenomenon results

from the two approaching spherical surfaces as the lubricant experiences normal pressures.

One method to evaluate the forces that develop at the spherical joints due to the squeeze-film effect is to use the Reynold's equation. Pinkus and Sternlicht [51], among others, have presented a detailed derivation of the Reynold's equation, which can be extended from the Navier-Stokes' equation. The Reynold's equation involves viscosity, density and fluid thickness as main parameters. The Reynold's equation, in general, can be used to evaluate the ball trajectory inside the socket for an external applied load. However in the present work, instead of knowing the applied load, the relative ball-socket motion characteristics are known from the multibody system dynamics and the fluid force from the pressure distribution in the lubricant is the quantity that has to be determined.

A simple alternative way to evaluate the lubrication forces developed in a spherical joint with lubricant is to equate the pressure flow to the pressure that results from displacement associated with the geometric configuration of the spherical joint elements. The configuration considered here is of a hemispherical seat which, owing to symmetry, has a cross section identical to that of Fig. 3.

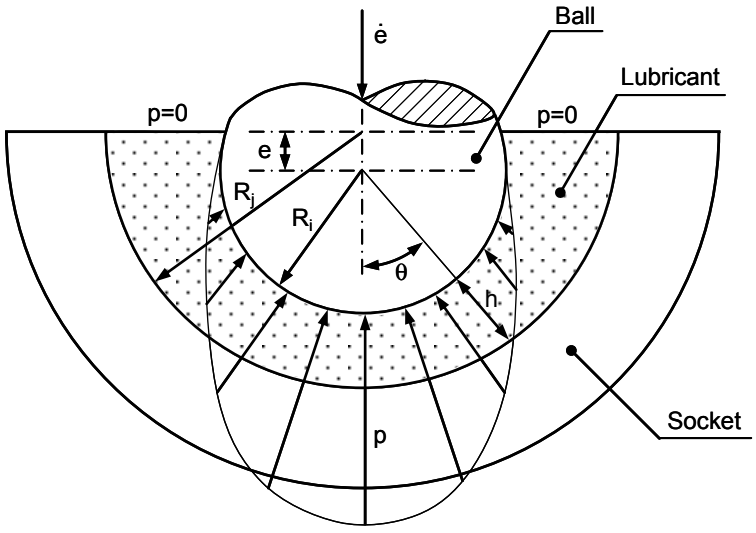

Figure 3. Generic representation of a spherical lubricated joint with squeeze-film.

Based on fundamental principles, Pinkus and Sternlicht [51] demonstrated that, for a spherical joint with lubricant, the amount of fluid that passes a conical element surface is given by,

$$Q = -\frac{\pi R_i \sin\theta h^3}{6\mu R_i}\frac{dp}{d\theta} \tag{16}$$

where R_i is the ball radius, h represents the thickness of the film lubricant, μ is the dynamic lubricant viscosity, θ is the angular coordinate and p is the pressure. The negative sign of Eq. (16) reflects the fact that the fluid flows down the pressure gradient. This is a characteristic of a fully developed pressure or Poisseuille pressure, i.e., it represents the flow of the fluid from regions of higher pressures to the regions of lower pressures [46, 47]. In addition, from the geometry of a spherical joint the fluid film thickness can be expressed as follows,

$$h = c(1-\varepsilon\cos\theta) \tag{17}$$

in which the eccentricity ratio, ε, is given by,

$$\varepsilon = \frac{e}{c} \tag{18}$$

with e and c being the magnitudes of the eccentricity and radial clearance, respectively.

On the other hand, based on the geometry of Fig. 3, the flow at any angle θ due to the radial velocity, $\dot{R}$, is expressed as [51],

$$Q = \pi\dot{R}R_i^2\sin^2\theta \tag{19}$$

where $\dot{R}$ is the velocity of the ball center that is responsible for the squeeze-film action, i.e., $\dot{R} = dh/dt$. This parameter can be evaluated by differentiating Eq. (4) with respect to time. Equation (19) corresponds the total flow rate through the spherical joint, and hence, it represents the amount of fluid that flows through the joint and is required to ensure a desired fluid thickness equal to h.

Thus, for the flow continuity, combining Eqs. (16)-(19) results the general expression for pressure gradient dp as follows,

$$dp = \frac{6\mu \dot{\alpha} \sin\theta}{(c/R_i)^3 R_i (1-\varepsilon\cos\theta)^3} d\theta \tag{20}$$

Then, the pressure distribution in the lubricated spherical joint can be obtained if Eq. (20) is integrated with an appropriate set of boundary conditions. In this particular issue, it is important to point out the two main types of boundary conditions are usually considered in the integrating process of Eq. (20). Equation (20) can be integrated either in the entire domain or half domain. These two types of boundary conditions, associated with the pressure field, correspond, respectively, to Sommerfeld's and Gümbel's boundary conditions [47]. In the later case, the pressure field is integrated only over the positive part by setting the pressure in the remaining portion equal to zero. In fact, the complete or full film does not take into account the cavitation phenomenon and, consequently, contemplate the existence of negative pressures. This case is however not realized in many applications due to the fluid incapacity to sustain significant sub-ambient pressures. In short, the following boundary conditions of the lubricant flow are used in the present study [51],

$$p(\pm\pi/2) = 0 \tag{21}$$

Thus, the pressure distribution can be obtained by integrating Eq. (20) and considering the boundary conditions of Eq. (21), yielding,

$$p = \frac{3\mu \dot{\alpha}}{(c/R_i)^3 R_i \varepsilon}\left[\frac{1}{(1-\varepsilon\cos\theta)^2} - 1\right] \tag{22}$$

Finally, the resulting squeeze F_S film force on the ball, which should be applied to equilibrate the fluid pressure, can be evaluated as the integral of the pressure field over a hemisphere, that is,

$$F_S = 2\pi R_i^2 \int_0^{\pi/2} p \sin\theta\cos\theta d\theta \tag{23}$$

from which,

$$F_S = \frac{6\pi\mu \dot{\alpha} R_i}{(c/R_i)^3}\left[\frac{1}{\varepsilon^3}\ln(1-\varepsilon) + \frac{1}{\varepsilon^2(1-\varepsilon)} - \frac{1}{2\varepsilon}\right] \tag{24}$$

In short, this illustrates that the squeeze lubricant forces at any instant of time can be evaluated in terms of the instantaneous eccentricity and relative radial velocity, as well as the constant parameters of the fluid viscosity, joint clearance and the ball radius. The direction of the squeeze force is collinear with the line of centers of the socket and ball, which is described by the eccentricity vector in Eq. (1). Thus the squeeze force can be introduced into the equation of motion of a multibody system as generalized forces, with the socket and ball centers as points of action for the force and reaction force, respectively. It is important to note that for high speed rotating machinery the lubricant viscous effect due to rotation also needs to be considered and included in the analysis. One possible methodology that must be followed to account for both wedge-film and squeeze-film effect is the one proposed by Goenka [44]. This, work presents the details of the Reynold's equation for the more general lubricated circumstances of a spherical joint with lubrication. Then, in a similar manner the resulting lubrication force in both radial and tangential directions developed should be introduced into the equations of motion of the mechanical system under analysis.

4. Results and discussion

In this section, an application example is used to assess the effectiveness of the proposed methodologies for modeling spherical joints in a multibody mechanical system in spatial motion. A four bar mechanism, depicted in Fig. 4, is selected for the study and for which a non-ideal spherical joint exists between the coupler and rocker bodies [52, 53]. In the present study, this particular joint is modeled as clearance joint with and without lubricant. The remaining revolute and spherical joints are considered to be ideal joints. Due to the existence of a joint clearance, the system has a total of five degrees of freedom. In order to keep the analysis simple, the bodies are assumed to be rigid. The numbers of the bodies and their corresponding local coordinate systems are illustrated in Fig. 4. The geometrical and inertial properties of the bodies that constitute the four bar mechanism are listed in Tab. 1.

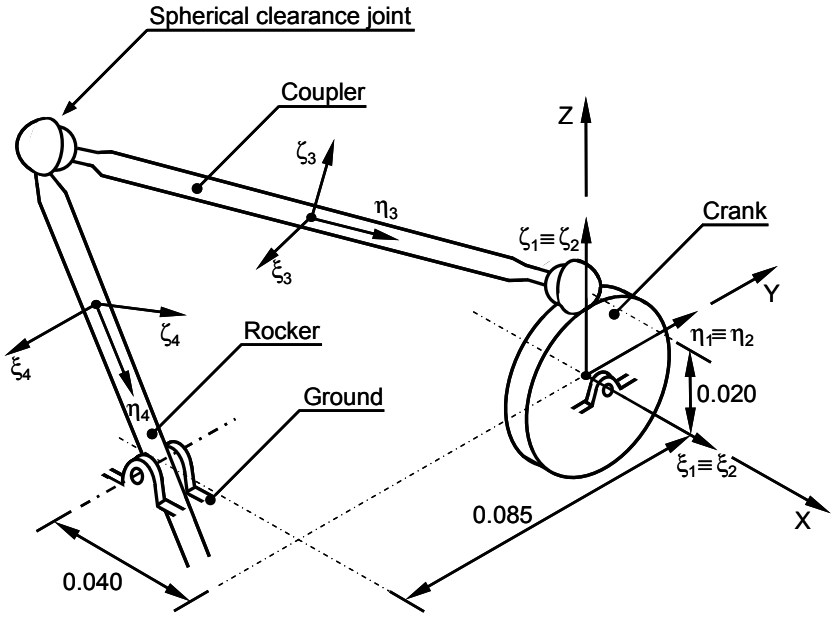

Figure 4. Schematic representation of the spatial four bar mechanism, which includes a non ideal spherical joint between the coupler and rocker.

Table 1. Geometrical and inertial properties of the spatial four bar mechanism.

Body Nr.	Length [m]	Mass [kg]	Moment of inertia [kgm^2]		
			$I_{\xi\xi}$	$I_{\eta\eta}$	$I_{\zeta\zeta}$
2	0.020	0.0196	0.0000392	0.0000197	0.0000197
3	0.122	0.1416	0.0017743	0.0000351	0.0017743
4	0.074	0.0316	0.0001456	0.0000029	0.0001456

In the dynamic simulation of this four bar mechanism, the system is released from rest corresponding to the initial configuration illustrated in Fig. 4. Furthermore, initially the socket and the ball centers are coincident. The acceleration due to gravity is taken as acting in the negative *Z*-direction. Hence, the dynamic behavior of the system is affected by the potential energy associated with the heights of centers of mass of all bodies. The main parameters used for the computational simulations of the system with ideal, dry and lubricated spherical joints and for the numerical methods required to solve the system dynamics are presented in Tab. 2.

Table 2. Parameters used in the dynamic simulation of the spatial four bar mechanism.

Nominal socket radius	10.0 mm
Nominal ball radius	9.8 mm
Radial clearance	0.2 mm
Restitution coefficient	0.9
Poisson's ration	0.3
Young's modulus	207 GPa
Lubricant viscosity	400 cP
Baumgarte stabilization parameters – α, β	5
Integrator algorithm	Gear
Integration time step	0.00001 s

In what follows, dynamic and kinematic results are presented and analyzed with the intent to demonstrate the performance of the four bar mechanism described above. This performance is quantified by plotting the reaction forces that develop at the spherical clearance joint and the relative motion between the socket and ball produced during the overall system's motion. When the spherical joint is modeled as dry joint, the intra-joint forces are evaluated by using Eq. (15), while for the case of lubricated model the reaction forces are computed by employing Eq. (24). In addition, the positions, velocities and accelerations of the rocker link in the *Z*-direction are also presented. Finally, the system's behavior is studied by the plots of some phase space portraits, namely those that relate the rocker velocity and rocker position, and the rocker

acceleration to the rocker velocity. The global results are compared with those obtained when the system is modeled with ideal joints only. The system's response with perfect joints is in accordance with the outcomes available in the literature [52].

The joint reaction forces that are developed at the spherical joints for the dry and lubricated models are plotted in Fig. 5, from which it can be observed that the dry joint model produces higher peaks. This is due to the fact that the socket and ball surfaces undergo successive direct collisions with each other and the impulsive forces associated with this type of contact are transmitted throughout the system. The presence of fluid lubricant between the socket and ball surfaces avoids this situation and acts like a damper element, which ultimately causes lower peaks in the joint reaction forces. In this case, the joint elements are apart from each other owing to the squeeze-film action. The difference in the relative positions of the socket and ball surfaces for the dry and lubricated spherical models is quite visible in the charts of Fig. 6. For the dry model, a period of impacts is immediately followed by rebounds, after which the ball tends to be in a continuous or permanent contact with the socket surface. In this phase, the relative deformation varies in the circumferential direction. In turn, the case of lubricated spherical model, the ball surface never reaches the socket due to the opposed action of the fluid, as observed in Fig. 6(b). In the present example, the radial clearance size is 0.2 mm.

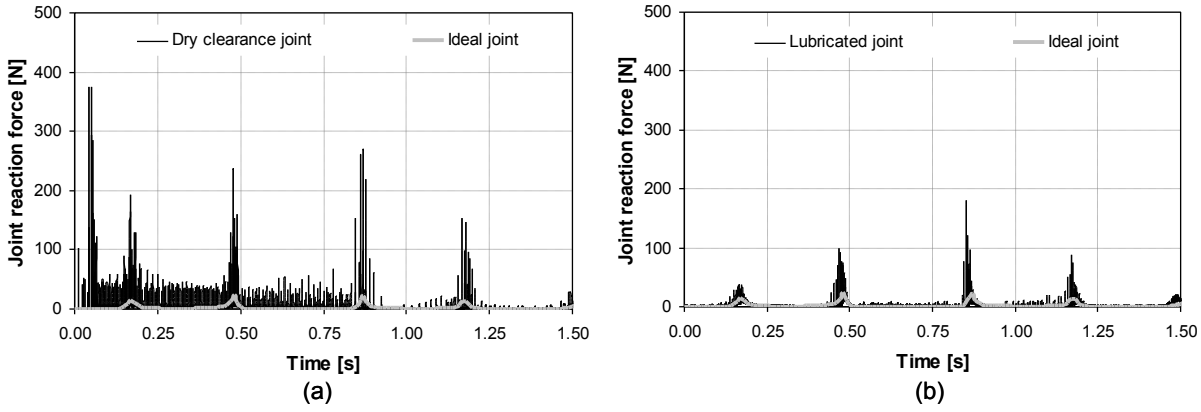

Figure 5. Joint reaction forces developed at the spherical clearance joint: (a) Dry joint model; (b) Lubricated joint model.

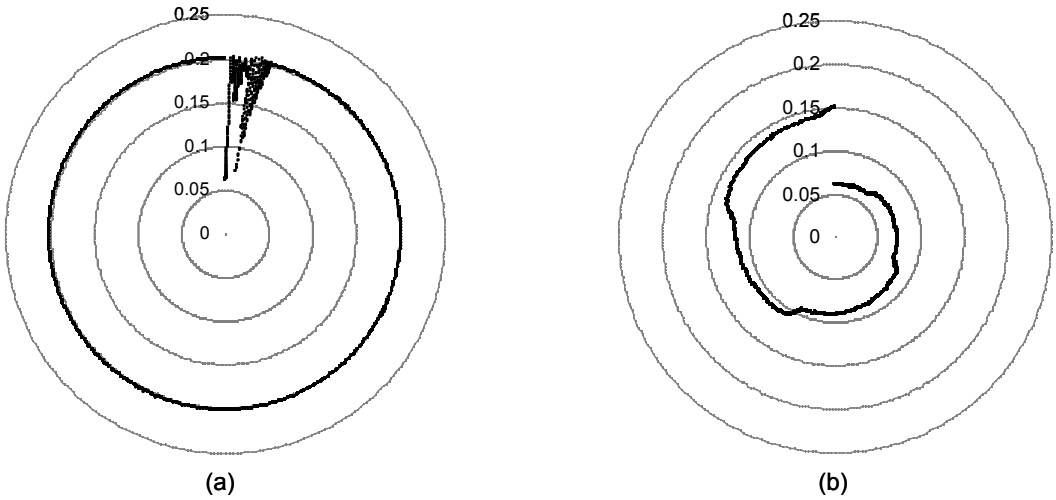

Figure 6. Eccentricity evolution with time: (a) Dry joint model; (b) Lubricated joint model.

Figure 7 shows the Z-component for the position, velocity and acceleration of the center of mass of rocker, for both dry and lubricated joints models. By observing Figs. 7(a) and 7(d), it can be concluded that the position accuracy of the four bar mechanism is significantly affected by the way the joint is modeled. This system is particularly sensitive to the spherical joint model because it does not include any external drivers other than the gravitational effect supplied to the system. Again, the levels of the impacts that take place at the dry clearance joints are quite visible in the jumps of the velocity and acceleration diagrams. Figure 7 also indicates that the four bar mechanism with dry spherical joint produces significantly larger velocities and accelerations on the system than those observed from the lubricated model. The system's response for the spherical lubricated case tends to be closer to the ideal situation since the presence of the fluid lubricant acts as a vibration absorber.

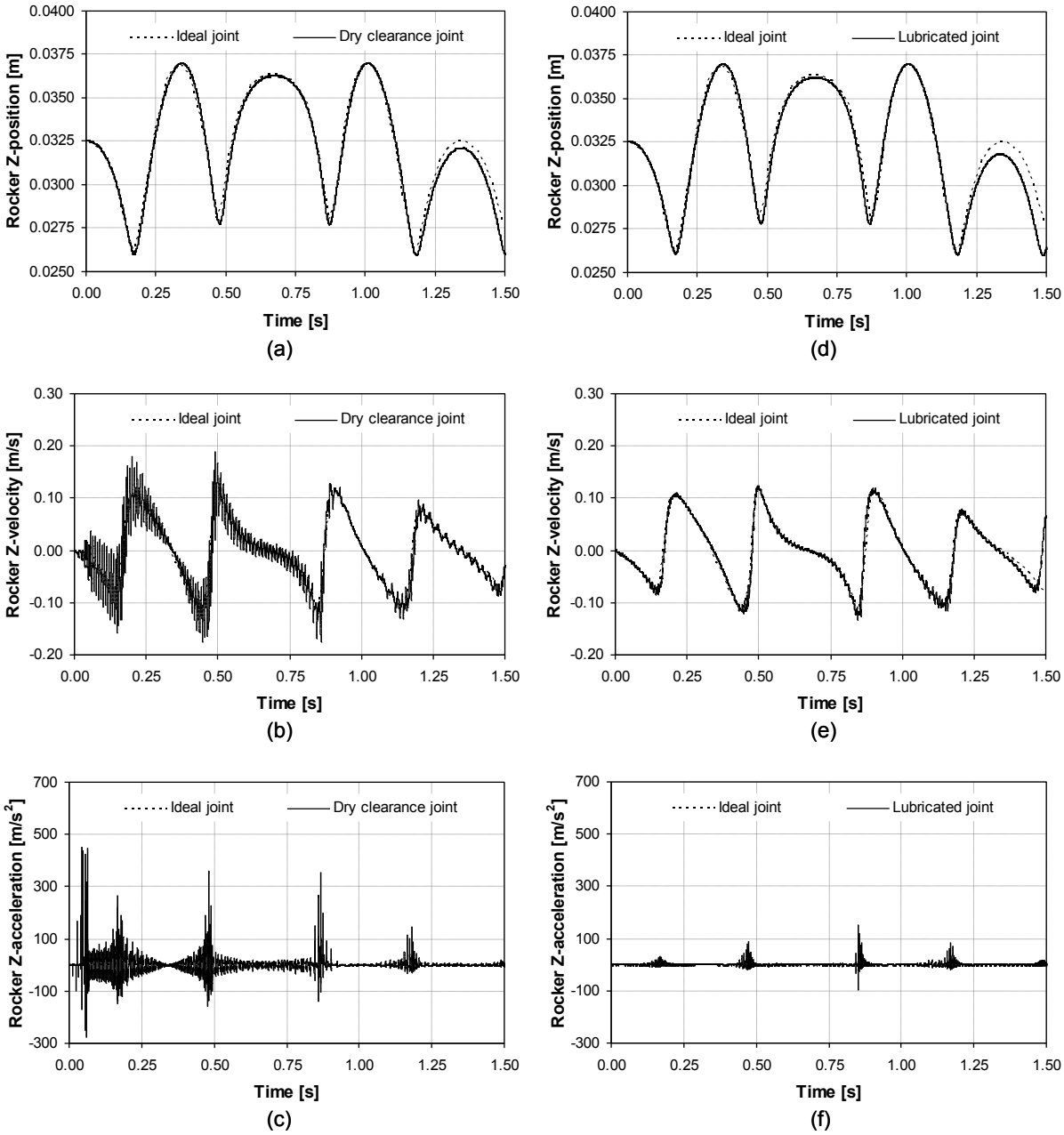

Figure 7. Z-position, Z-velocity and Z-acceleration of the rocker center of mass: (a)-(c) Dry joint model; (d)-(f) Lubricated joint model.

In order to better study the nonlinear nature behavior of the four bar mechanism, two phase space portraits for different joint models are developed and presented in Figs. 8(b) and 8(e). The systems response tends to be highly nonlinear for the dry case, since the relation motion between the socket and ball can change from free flights to impact and continuous contact. This causes a more complex and denser aspect in the phase space portraits, which is a clear and strong indicator of chaotic behavior. Once again,

the system response with lubricated joint, Figs. 8(c), (f), exhibits is closer to the case of ideal joints due to the fact that the fluid action acts like a filter by reducing the level of peaks due to severe dry impacts. This phenomenon is visible by the simpler and less chaotic plots of the phase space portraits.

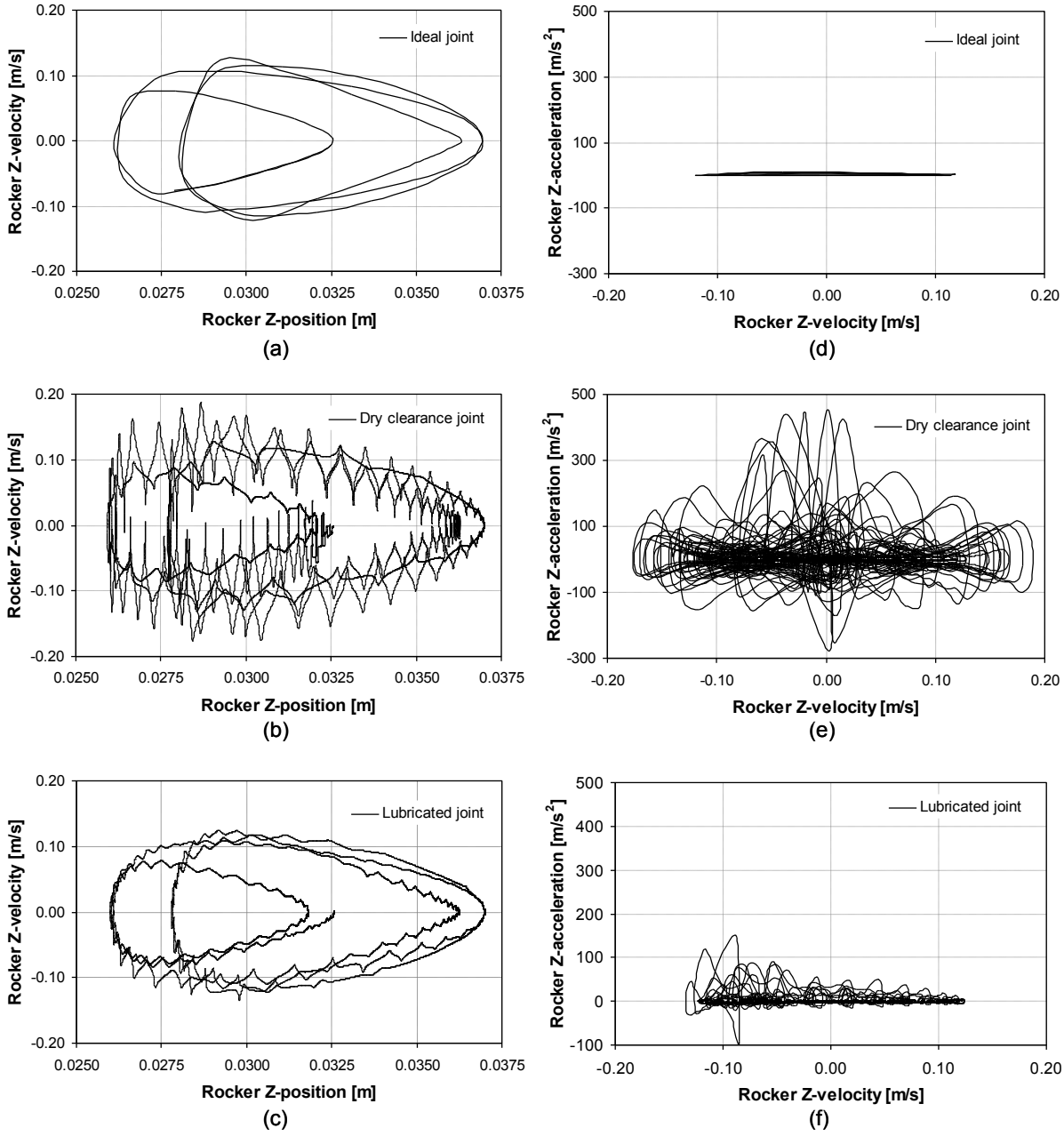

Figure 8. Phase space portraits for different joint models: (a)-(c) Z-rocker velocity versus Z-rocker position; (d)-(f) Z-rocker acceleration versus Z-rocker velocity.

Figure 9 shows the influence of the clearance size on the system's response for the case of dry contact model. The plots are those of the Z-rocker velocity. In this particular analysis, four clearance sizes are considered, namely, 0.2, 0.15, 0.1 and 0.075 mm. As it was expected, the system's response tends to converge to the case of ideal when the clearance size is decreased. This observation is logical since the level impacts that occur between ball and socket surfaces tend to become lower for the small clearances. This type of analysis can be useful in the design of mechanical system, namely in what concerns to the selection of the proper clearance size for the joints.

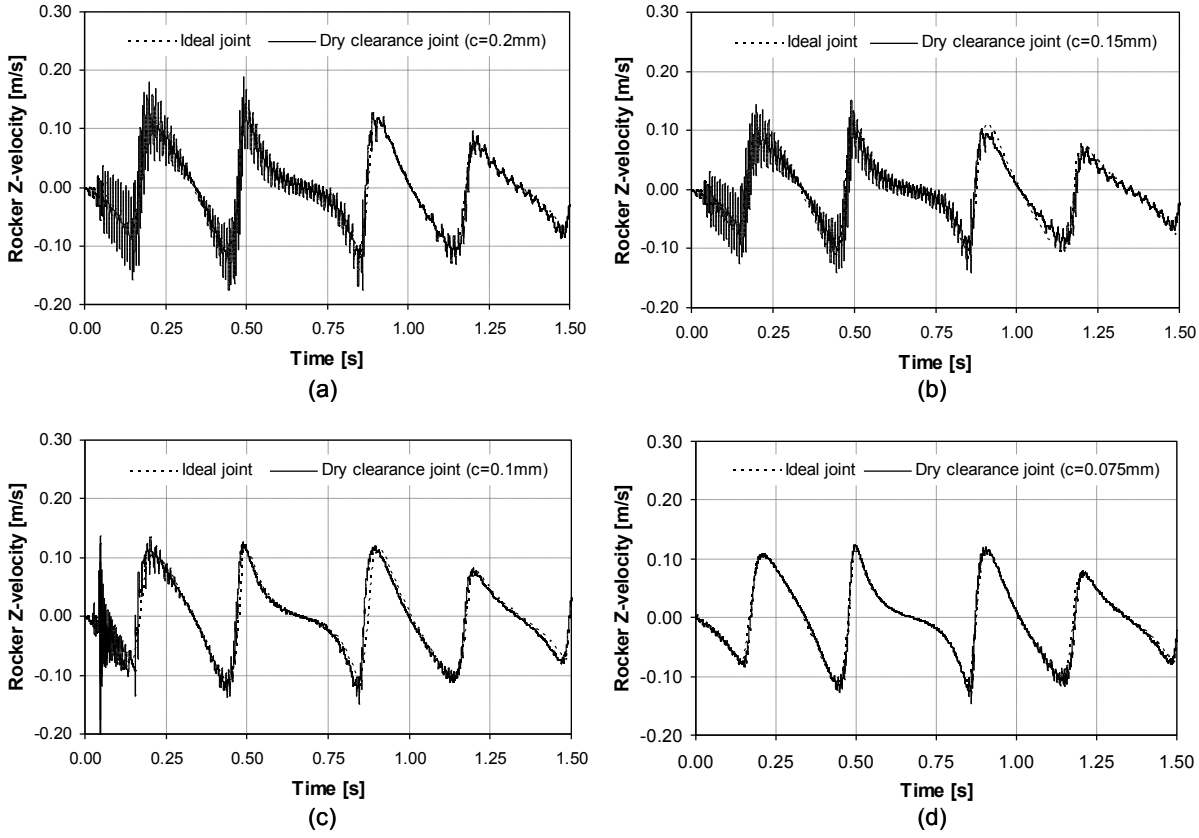

Figure 9. Influence of the clearance size on the Z-rocker velocity of the four bar mechanism: (a) *c*=0.2 mm; (b) *c*=0.15 mm; (c) *c*=0.1 mm; (d) *c*=0.075 mm.

It must be noted that from a physical point of view, the system's response dependens on the material properties involved in the contact process. Figure 10 shows the plots of the he Z-rocker velocity for two different values of restitution coefficient, namely 0.9 and 0.5. By analyzing the plots of Fig. 10, it can be observed how the Z-rocker velocity is affected by the values of restitution coefficient. The rebounds are at lower levels when the restitution coefficient decreases. Lower value for the coefficient of restitution corresponds to higher level of energy dissipation in the contact process, as it is evident in Fig. 10b.

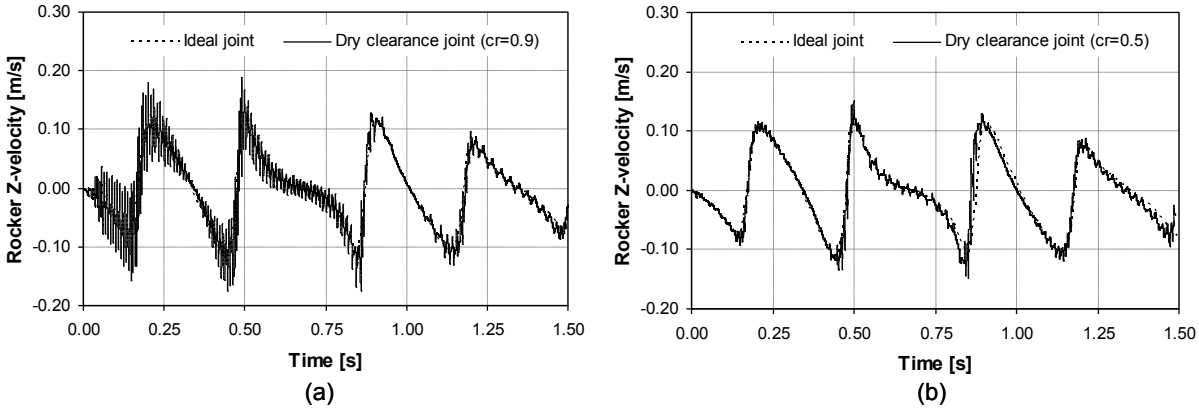

Figure 10. Influence of the restitution coefficient on the Z-rocker velocity of the four bar mechanism: (a) c_r=0.9; (b) c_r=0.5.

One important issue associated with the modeling and simulation of any multibody system is its computational efficiency. This is particularly relevant when the systems include contact-impact events, such as in the case of realistic joints. For the topics studied in the present work, it is convenient to relate them with the necessary computational effort. For the data listed in Tab. 2, and for analyses for the ideal case, dry contact and lubricated spherical joints, the computation times for the simulations were 47s, 67s and 540s, respectively. In case of ideal joints it is necessary to evaluate the functions associated with the kinematic constraints, which involves an iterative procedure to solve them. When the joint is a dry clearance model, the constraints are eliminated and the contact forces are the only quantities to be computed, which is a straightforward task. In this case, when there is no contact, there is no force to be evaluated. Finally, for the case lubricated joints, the lubrication forces that are always acting on the system have to be calculated at each time step, and hence the computation time is the largest.

5. Conclusions

The main objective of the work presented in this paper is to contribute to the improvement of the methodologies dealing with the analysis of realistic spatial multibody systems, which include imperfect or real joints. These are joints in which the effects of clearance and lubrication are taken into account in the multibody systems formulation. The methodology developed here incorporates the contact-impact forces due to the collisions of the bodies that constitute the spatial spherical clearance joints into the equations of the motion that govern the dynamic response of the multibody mechanical systems. A continuous contact force model is utilized which provides the intra-joint due to dry contact and lubrication forces that develop during the normal operations of the mechanisms. The effect of lubrication in spherical clearance joint is considered by the squeeze film providing pressure or force in the radial joint direction. Thus, a suitable model for spherical clearance joints is embedded into the multibody systems methodology. The methodology is easy and straightforward to implement in a computational code because resultant forces due to the fluid action are in explicit forms.

As application, a spatial four bar mechanism was considered here with a spherical clearance joint. The system was driven by the gravitational effects only. The positions and velocities of the mechanical system with clearance modeled with dry contact and with lubrication were compared to those from system with ideal joints. The existence of a non-ideal joint in the system significantly increases the amount of dissipated energy. Furthermore, the fluid lubricant acts as a nonlinear spring-damper in so far as lubricated spherical bearing absorbs some of the energy produced by the rocker. The lubricant introduces effective stiffness and damping to the four bar mechanism, which plays an important role in the stability of the mechanical components.

Finally, it should be highlighted that the results presented in this paper represent an upper bound of the joint reaction forces and rocker kinematics due to the existence of realistic joints, since the elasticity of the links was not included in the analysis. This effects tends to reduce the joint reaction forces and rocker kinematics. Using the methodologies presented in this paper, the effects of clearance and lubrication in spherical joints can be effectively studied.

Acknowledgments

The authors would like to thank the Portuguese Foundation for Science and Technology (FCT) for the support given through projects ProPaFe - Design and Development of a Patello-Femoral Prosthesis (PTDC/EME-PME/67687/2006).

References

1. Flores, P., Ambrósio, J., Claro, J.C.P., Lankarani, H.M.: Kinematics and Dynamics of Multibody Systems with Imperfect Joints: Models and Case Studies. In Lecture Notes in Applied and Computational Mechanics Vol. 34, Berlin Heidelberg New-York, Springer-Verlag, (2008).
2. Crowthera, A.R., Singha, R., Zhangb, N., Chapman, C.: Impulsive response of an automatic transmission system with multiple clearances: Formulation, simulation and experiment. Journal of Sound and Vibration, 306, 444-466, (2007).
3. Erkaya S. Uzmay I.: A neural-genetic (NN–GA) approach for optimising mechanisms having joints with clearance. Multibody System Dynamics, 20(1), 69-83, (2008).
4. Ishida, Y., Inagaki, M., Ejima, R., Hayashi, A.: Nonlinear resonances and self-excited oscillations of a rotor caused by radial clearance and collision. Nonlinear Dynamics, (2009). DOI: 10.1007/s11071-009-9482-3
5. Erkaya, S., Uzmay, I., Investigation on effect of joint clearance on dynamics of four-bar mechanism. Nonlinear Dynamics, (2009). DOI: 10.1007/s11071-009-9470-7
6. Duarte, F.B., Tenreiro, J.: Describing function of two masses with backlash: Nonlinear Dynamics, 56(4), 409-413, (2009).
7. Park, J., Nikravesh, P.E.: Effect of Steering-Housing Rubber Bushings on The Handling of a Vehicle. SAE Paper 970103, SAE, Warrendale, Pennsylvania, 1997).
8. Ambrósio, J., Veríssimo, P.: Sensitivity of a vehicle ride to the suspension bushing characteristics. Journal of Mechanical Science and Technology, 23, 1075-1082, (2009).

9. Smith, S.L., Dowson, D., Goldsmith, A.A.J.: The effect of diametral clearance, motion and loading cycles upon lubrication of metal-to-metal total hip replacements. Proc. Inst. Mech. Eng. J. Mech. Eng. Sci., 215, 1-5, (2001).
10. Dowson, D., Hardaker, C., Flett, M., Isaac, G.H.: A Hip Joint Simulator Study of the Performance of Metal-on-Metal Joints: Part I: The Role of Materials. The Journal of Arthroplasty, 19(8), 118-123, (2004).
11. Fialho, J.C., Fernandes, P.R., Eça, L., Folgado, J.: Computational hip joint Simulator for wear and heat generation. Journal of Biomechanics, 40, 2358-2366, (2007).
12. Dubowsky, S., Freudenstein, F.: Dynamic Analysis of Mechanical Systems with Clearances, Part 1: Formulation of Dynamic Model. Journal of Engineering for Industry, 93(1), 305-309, (1971).
13. Dubowsky, S.: On Predicting the Dynamic Effects of Clearances in One-Dimensional Closed Loop Systems. Journal of Engineering for Industry, 96(1), 324-329, (1974).
14. Earles, S.W.E., Wu, C.L.S.: Motion Analysis of a Rigid Link Mechanism with Clearance at a Bearing Using Lagrangian Mechanics and Digital Computation. Mechanisms, 83-89, (1973).
15. Grant, S.J., Fawcett, J.N.: Effects of Clearance at the Coupler-Rocker Bearing of a 4-Bar Linkage. Mechanism and Machine Theory, 14, 99-110, (1979).
16. Haines, R.S.: Survey: 2-Dimensional Motion and Impact at Revolute Joints. Mechanism and Machine Theory, 15, 361-370, (1980).
17. Towsend, M.A., Mansour, W.M.: A Pendulating Model for Mechanisms with Clearances in the Revolutes. Journal of Engineering for Industry, 97(2), 354-358, (1975).

18. Miedema, B., Mansour, W.M.: Mechanical Joints with Clearance: a Three Mode Model. Journal of Engineering for Industry, 98(4), 1319-1323, (1976).
19. Haines, R.S.: A Theory of Contact Loss at Resolute Joints with Clearance. Proceedings of Institution of Mechanical Engineers, Journal of Mechanical Engineering Science, 22(3), 129-136, (1980).
20. Bengisu, M.T., Hidayetoglu, T., Akay, A.: A Theoretical and Experimental Investigation of Contact Loss in the Clearances of a Four-Bar Mechanism. Journal of Mechanisms, Transmissions, and Automation Design, 108, 237-244, (1986).
21. Feng, B., Morita, N., Torii, T.: A New Optimization Method for Dynamic Design of Planar Linkage with Clearances at Joints – Optimizing the Mass Distribution of Links to Reduce the Change of Joint Forces. Journal of Mechanical Design, 124, 68-73, (2002).
22. Orden, J.C.G.: Analysis of Joint Clearances in Multibody Systems. Multibody System Dynamics, 13(4), 401-420, (2005).
23. Winfrey, R.C., Anderson, R.V., Gnilka, C.W.: Analysis of Elastic Machinery with Clearances. Journal of Engineers for Industry, 95, 695-703, (1973).
24. Dubowsky, S., Gu, P.Y., Deck, J.F.: The Dynamic Analysis of Flexibility in Mobile Robotic Manipulator Systems. Proceedings of VIII World Congress on the Theory of Machines and Mechanisms, Prague, Czechoslovakia. August 26-31, 12p, (1991).
25. Bauchau, O.A., Rodriguez, J.: Modelling of Joints with Clearance in Flexible Multibody Systems. International Journal of Solids and Structures, 39, 41-63, (2002).
26. Dubowsky, S., Moening M.F.: An Experimental and Analytical Study of Impact Forces in Elastic Mechanical Systems with Clearances. Mechanism and Machine Theory, 13, 451-465, (1978).

27. Kakizaki, T., Deck, J.F., Dubowsky, S.: Modeling the Spatial Dynamics of Robotic Manipulators with Flexible Links and Joint Clearances. Journal of Mechanical Design, 115, 839-847, (1993).
28. Liu, C., Zhang, K. and Yang, L.: Normal Force-Displacement Relationship of Spherical Joints with Clearances. Journal of Computational and Nonlinear Dynamics, 1(2), 160-167, (2006).
29. Flores, P., Ambrósio, J., Claro, J.C.P., Lankarani, H.M.: Dynamics of Multibody Systems with Spherical Clearance Joints. Journal of Computational and Nonlinear Dynamics, 1(3), 240-247, (2006).
30. Nikravesh, P.E.: Computer Aided Analysis of Mechanical Systems. Prentice Hall, Englewood Cliffs, (1988).
31. Shabana, A.A.: Dynamics of Multibody Systems, John Wiley and Sons, New York, (1989).
32. Baumgarte, J.: Stabilization of Constraints and Integrals of Motion in Dynamical Systems. Computer Methods in Applied Mechanics and Engineering, 1, 1-16, (1972).
33. Flores, P., Seabra, E.: Influence of the Baumgarte parameters on the dynamics response of multibody mechanical systems. Dynamics of Continuous, Discrete and Impulsive Systems, Series B: Applications and Algorithms, 16(3), 415-432, (2009).
34. Nikravesh, P.E.: Initial condition correction in multibody dynamics. Multibody System Dynamics, 18, 107-115, (2007).
35. Gear, C.W.: Numerical Initial Value Problems in Ordinary Differential Equations. Prentice-Hall, Englewood Cliffs, New Jersey, (1971).
36. Shampine, L., Gordon, M.: Computer Solution of Ordinary Differential Equations: The Initial Value Problem. Freeman, San Francisco, California, (1972).

37. Flores P., Ambrósio J., Claro J.C.P., Lankarani H.M., Koshy C.S.: A study on dynamics of mechanical systems including joints with clearance and lubrication. Mechanism and Machine Theory, 41(3), 247-261, (2006).

38. Ahmed, S., Lankarani, H.M., Pereira, M.F.O.S.: Frictional Impact Analysis in Open Loop Multibody Mechanical System. Journal of Mechanical Design, 121, 119-127, (1999).

39. Hertz, H.: On the contact of solids - On the contact of rigid elastic solids and on hardness. (Translated by D. E. Jones and G. A. Schott), Miscellaneous Papers, Macmillan and Co. Ltd., London, England, 146-183, (1896).

40. Goldsmith, W.: Impact - The theory and physical behaviour of colliding solids. Edward Arnold Ltd, London, England, (1960).

41. Lankarani, H.M., Nikravesh, P.E.: A contact force model with hysteresis damping for impact analysis of multibody systems. Journal of Mechanical Design, 112, 369-376, (1990).

42. Lankarani, H. M., Nikravesh, P. E.: Continuous Contact Force Models for Impact Analysis in Multibody Systems. Nonlinear Dynamics, 5, 193-207, (1994).

43. Boker, J.F.: Dynamically Loaded Journal Bearings: Mobility Method of Solution. Journal of Basic Engineering, 537-546, (1965).

44. Goenka, P.K.: Effect of Surface Ellipticity on Dynamically Loaded Spherical and Cylindrical Joints and Bearings. PhD Dissertation, Cornell University, Ithaca, New York, (1980).

45. Goenka, P.K., Dynamically Loaded Journal Bearings: Finite Element Method Analysis. Transactions of the ASME, Journal of Tribology, 106, 429-439, (1984).

46. Hamrock, B.J.: Fundamentals of Fluid Film Lubrication. McGraw Hill, New York, (1994).

47. Frêne, J., Nicolas, D., Degneurce, B., Berthe, D., Godet, M., Hydrodynamic Lubrication - Bearings and Thrust Bearings, Elsevier, Amsterdam, The Netherlands, (1997).

48. Hirani, H., Athre, K., Biswas, S.: Rapid and globally convergent method for dynamically loaded journal bearing design. Proceedings of the Institution of Mechanical Engineers, Part J, Engineering Tribology, 212,(3), 207-214, (1998).

49. Hlavácek, M., Squeeze-Film Lubrication of the Human Ankle Joint Subjected to the Cyclic Loading Encountered in Wlaking. Journal of Tribology, 127, 141-148, (2005).

50. Wang, F., Jin., Z.: Transient Elastohydrodynamic lubrication of Hip Joint Implants. Journal of Tribology, 130, 011007-11, (2008).

51. Pinkus, O., Sternlicht, S.A.: Theory of Hydrodynamic Lubrication, McGraw Hill, New York, (1961).

52. Haug E.J.: Computer-Aided Kinematics and Dynamics of Mechanical Systems. Volume I: Basic Methods, Allyn and Bacon, Boston, Massachusetts, (1989).

53. Flores, P., Dynamic Analysis of Mechanical Systems with Imperfect Kinematic Joints, Ph.D. Dissertation, University of Minho, Guimarães, Portugal, (2005).